research papers

In situ system for X-ray absorption spectroscopy experiments to investigate nanoparticle crystallization

C. T. Meneses,[a,b]* **W. H. Flores,**[a] **A. P. Sotero,**[b] **E. Tamura,**[b] **F. Garcia**[b] **and J. M. Sasaki**[a]

[a]Departamento de Física, Universidade Federal do Ceará, Campus do Pici, CP 6030, 60455-760 Fortaleza, CE, Brazil, and [b]Laboratório Nacional de Luz Síncrotron, CP 6192, CEP 13084-971, Campinas, SP, Brazil. E-mail: cristiano@fisica.ufc.br

A new furnace, based on a halogen lamp, and a sample cell have been designed and constructed for *in situ* X-ray absorption spectroscopy experiments in conventional and dispersive mode (transmission and fluorescence geometries). The main application of the apparatus is thermal treatment studies under controlled conditions for dynamical processes. The sol–gel (gelatin) method has been utilized to synthesize NiO nanoparticles. During this heating process, *in situ* Ni K-edge X-ray absorption near-edge structural measurements provided evidence of the evolution of a Ni environment until complete NiO nanoparticle crystallization. This case is reported in order to show the furnace performance in dispersive mode.

Keywords: instrumentation; *in situ* XAS; nanoparticles.

1. Introduction

In recent years X-ray absorption spectroscopy (XAS) has been used to study the structural properties of several materials (Koningsberger & Prins, 1988), especially those that display catalytic properties. Among this and others studies, several kinds of cells have been developed, *e.g.* high pressure (Betta *et al.*, 1984), electrochemical (Braun *et al.*, 2003), catalysis cell (Girardon *et al.*, 2005; Pettiti *et al.*, 1999), furnaces for studying the synthesis of materials by X-ray absorption (Huwe & Fröba, 2004; Dent *et al.*, 1995) and X-ray diffraction (Geselbracht *et al.*, 2000; Puig-Molina *et al.*, 2001; Capitán *et al.*, 1999).

In general the furnaces quoted above were developed with resistance as the heating source. However, lately the halogen lamp (Zanetti *et al.*, 2001; Kimura *et al.*, 2000) and microwave furnaces (Gómez *et al.*, 2004; Marinel & Desgardin, 2001) have been used, especially for synthesis and kinetics studies. In particular, these systems have been proposed for the synthesis of nanoparticles and to control the growth of crystallites (Jia *et al.*, 2005).

In this paper we describe a compact furnace that has been developed with halogen lamps as heater elements for XAS experiments. It can be used in kinetics as well as phase-transition studies with thermal treatment up to 1000 K, with and without gas flux. A sample cell was built for the high-temperature regime in transmission–dispersive mode. The main advantages of this furnace are the possibility to perform measurements with different heating rates, the control of

cooling rates up to 60 K min^{-1}, and the efficient control of isothermals (plateaus) in the heating process. All apparatus was developed for experiments at the D06A-DXAS and D04B-XAFS beamlines of the Laboratório Nacional de Luz Síncrotron (LNLS), Campinas, Brazil. An example of the possible treatments will be shown below using dispersive X-ray absorption spectroscopy (DXAS).

2. Experimental apparatus

A schematic view of the furnace is shown in Fig. 1. The furnace is made up of three main parts: water-cooled stainless steel/ceramic block; heating element and temperature controller; and sample chamber. The ceramic block, covered by glass wool, is housed in a water-cooled stainless steel sheet (2 mm thick, giving total dimensions of 38 cm × 27 cm × 25 cm).
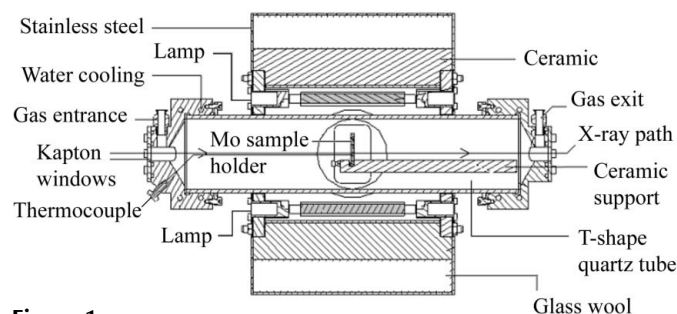

Figure 1
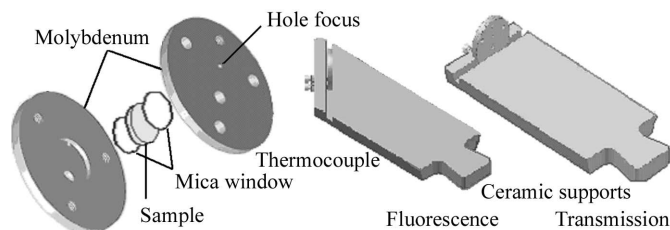Schematic of the furnace experimental set-up and components.

Figure 2
Experimental sample holder (room sample), molybdenum plates (left), and transmission and fluorescence ceramic supports (right).

The furnace operates using a commercial temperature controller (OMRON model E5CK with power module VARIX, 40 A/240 V) and twelve 500 W halogen lamps as the heating source. Temperature readout is carried out using a K-type thermocouple attached to the sample holder, which drives the thermal control system. A programmable system allows heating processes (ramps and plateaus) to be performed. The furnace can achieve 400 K in 2 min with temperature fluctuations about ±1 K using only 5% of the power. An example of these processes will be shown in the following section.

The sample room contains a T-shaped quartz tube (60 mm in diameter) with ends closed by aluminium flanges. The flanges are cooled by water and contain sealed Kapton windows which lie in the X-ray path. It is possible to evacuate and/or flow gases through the sample chamber. For the results of this paper, the sample was exposed to the room atmosphere. A ceramic basis is used to fix the sample cell; for instance, for fluorescence experiments a basis with an inclination of 45° to the direction of the quartz tube [Fig. 2 (right)] is used. A simple quartz tube of linear shape for measurements in transmission geometry is also available.

The cell in which the sample is fitted (sample cell) is fabricated from molybdenum plates. A drawing showing the sample cell is given in Fig. 2 (left). It consists of two plates that are tightly clamped together using screws and polished to obtain a good seal. At the junction of the two plates there is a cavity for holding the sample of desired thickness. On either side of the plates there is a hole (3 mm) for the X-ray beam, which is closed using mica windows. Thus, the sample is sandwiched between two mica windows (of thickness 25 μm) which can be changed to beryllium windows if necessary. This apparatus has the advantage that a sample can be heated rapidly for higher-heating-rate measurements. The sample region can be easily aligned in front of the beam by vertical translation, and the transmitted beam can be measured during thermal treatments. The disposable sample cell may also be fabricated from boron nitride ceramic.

3. Case application

XAS experiments were conducted on a metal/gelatin system by soft-chemical route. This route, under well controlled conditions (concentrations, pH, temperature and time), allows the formation of a stable inorganic/organic/NaCl system, the latter consisting of the mixture starting materials (Meneses, Flores, Garcia & Sasaki, 2006). The sample was pulverized, sieved to homogenize, and pressed into pellets with thicknesses in the micrometer range. After metal incorporation in the gelatin framework, the nanoparticle growth was investigated *in situ* during heat treatment. The results of nanoparticles NiO crystallization and structural phase transformations are presented below.

The measurements were obtained in transmission geometry using the dispersive mode at the D06A-DXAS beamline (Tolentino *et al.*, 2005). An X-ray beam with a bandwidth of a few hundred eV around the Ni K-edge (8333 eV) was selected using a curved Si(111) crystal monochromator. Its bending mechanism focused the beam at the sample position and the transmitted beam was collected using a CCD camera. For each measured spectrum an exposure time of 30 ms was used. In order to improve the signal-to-noise ratio, 50 accumulations (frames) compose a full spectrum with 1.5 s of total acquisition time. Conversion of data, pixel to energy, was performed by comparing measurements in conventional mode with those in dispersive mode from standard foils (Ni metal and NiO).

The temperature-programmed curve (ramps and plateaus) at the sample position during heating is shown in Fig. 3(*a*). This curve shows a good temperature control in the ramps as well as in the plateaus. It can be seen in the inset that the temperature fluctuations in the plateaus are about ±1 K. The heating and cooling rates in this case were 5 and 10 K min^{-1}, respectively.

Fig. 3(*b*) shows the most significant X-ray absorption near-edge structure (XANES) spectra recorded for the heating curve in Fig. 3(*a*). All spectra were normalized and the background was corrected for each spectrum following standard procedures. Each spectrum collected by the CCD detector is identified in the figure by the temperature and crystallization time. These spectra allow us to determine qualitatively the crystalline phase and the structural transformations during the heating process. Noticeable changes in the spectra are quite visible at 732 K, showing the appearance of the first oscillation (at 8361 eV), and were attributed to the initial stage of crystallization of NiO nanoparticles (Meneses, Flores, Garcia & Sasaki, 2006), with the crystallization becoming visible after 773 K through the increasing oscillations. These results may suggest the mechanism of nanoparticles growth, and that this XAS technique could be a promising technique for controlling nanoparticles size. A semi-quantitative analysis of all spectra will be published elsewhere (Meneses, Flores & Sasaki, 2006).

The NiO nanoparticles collected at the end of the heating process were characterized by performing Rietveld refinement on X-ray powder diffraction patterns (Fig. 3b, inset) obtained using a conventional X-ray diffractometer (Bragg–Brentano geometry). The particle size was calculated through the full width at half-maximum of the diffraction peaks using the well known Scherrer equation (Azároff, 1968). The crystallite size was estimated to be near to 15 nm.
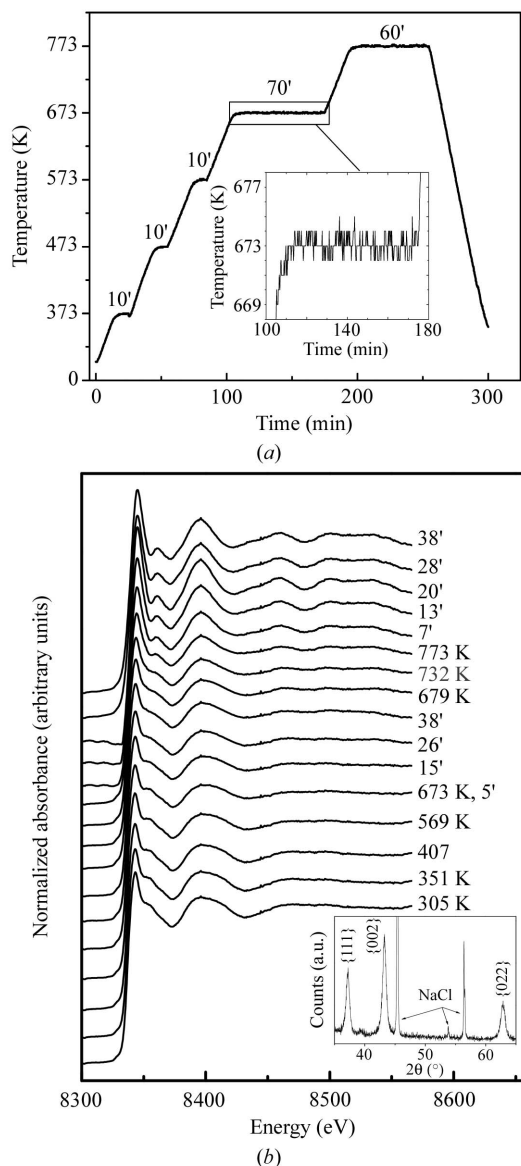
Figure 3
(a) Heating curve. (b) XANES spectra acquired during heating.

4. Conclusion

We have presented a new experimental set-up designed to study both transition and formation of phases under a dynamic process. In particular we have shown that the present system is helpful for studying the growth control of NiO nanoparticles during thermal treatment. The formation of these small particles of nanometer order can be attributed to break-up of Ni/gelatin framework through thermal treatment, which allows the Ni atoms to react with O_2 to form NiO.

References

Azároff, L. V. (1968). *Elements of X-ray Crystallography.* New York: McGraw-Hill.

Betta, R. A. D., Boudart, M., Foger, K., Löffler, D. G. & Sánchez-Arrieta, J. (1984). *Rev. Sci. Instrum.* **55**, 1910–1913.

Braun, A., Shrout, S., Fowlks, A. C., Osaisai, B. A., Seifert, S., Granlunde, E. & Cairns, E. J. (2003). *J. Synchrotron Rad.* **10**, 320–325.

Capitán, M. J., Thouin, N. & Rostaing, G. (1999). *Rev. Sci. Instrum.* **70**, 2248–2252.

Dent, A. J., Greaves, G. N., Roberts, M. A., Sankar, G., Wright, P. A., Jones, R. H., Sheehy, M., Madill, D., Catlow, C. R. A., Thomas, J. M. & Rayment, T. (1995). *Nucl. Instrum. Methods Phys. Res. B*, **97**, 20–22.

Geselbracht, M. J., Walton, R. I., Cowell, E. S., Millange, F. & O'Hareb, D. (2000). *Rev. Sci. Instrum.* **71**, 4177–4181.

Girardon, J.-S., Khodakov, A. Y., Capron, M., Cristol, S., Dujardin, C., Dhainaut, F., Nikitenko, S., Meneau, F., Brasc, W. & Payen, E. (2005). *J. Synchrotron Rad.* **12**, 680–684.

Gómez, I., Hernández, M., Aguilar, J. & Moisés, H. (2004). *Ceram. Int.* **30**, 893–900.

Huwe, H. & Fröba, M. (2004). *J. Synchrotron Rad.* **11**, 363–365.

Jia, Z., Kang, S., Shi, S., Nikles, D. E. & Harrell, J. W. (2005). *J. Appl. Phys.* **97**, 10J310.

Kimura, H., Jia, X., Shoji, K., Sakai, R. & Katsumata, T. (2000). *J. Cryst. Growth*, **212**, 364–367.

Koningsberger, D. C. & Prins, R. (1988). *X-ray Absorption: Principles, Applications, Techniques of EXAFS, SEXAFS and XANES*, Vol. 92, edited by J. D. Winefordner and I. M. Kolthoff, pp. 4–9. New York: Wiley-Interscience.

Marinel, S. & Desgardin, G. (2001). *J. Eur. Ceram. Soc.* **21**, 1919–1923.

Meneses, C. T., Flores, W. H., Garcia, F. & Sasaki, J. M. (2006). *J. Nanopart. Res.* Accepted.

Meneses, C. T., Flores, W. H. & Sasaki, J. M. (2006). In preparation.

Pettiti, I., Gazzoli, D., Inversi, M., Valigi, M., De Rossi, S., Ferraris, G., Porta, P. & Colonna, S. (1999). *J. Synchrotron Rad.* **6**, 1120–1124.

Puig-Molina, A., Gorges, B. & Graafsma, H. (2001) *J. Appl. Cryst.* **34**, 677–687.

Tolentino, H. C. N., Cezar, J. C., Watanabe, N., Piamonteze, C., Souza-Neto, N. M., Tamura, E., Ramos, A. Y. & Neueschwander, R. (2005). *Phys. Scr.* T**115**, 977–979.

Zanetti, S. M., Bueno, P. R., Leite, E., Longo, E. & Varela, J. A. (2001). *J. Appl. Phys.* **89**, 3416–3419.